

**CHEMICAL
RESEARCH,
DEVELOPMENT &
ENGINEERING
CENTER**

DTIC FILE COPY

CRDEC-TR-251

**SPECTROSCOPIC ANALYSES AND PERFORMANCE
OF COPPER/ZINC IMPREGNATED, ACTIVATED CARBONS**

AD-A231 693

**DTIC
ELECTE
FEB 08 1991
S B D**

**Erica Peterson
Robert Morrison**

PHYSICAL PROTECTION DIRECTORATE

**Michelle Farris
Joseph Rossin**

**GEO-CENTERS, INC.
Fort Washington, MD 20744**

December 1990

**U.S. ARMY
ARMAMENT
MUNITIONS
CHEMICAL COMMAND**



Aberdeen Proving Ground, Maryland 21010-8423

DISTRIBUTION STATEMENT A

**Approved for public release;
Distribution Unlimited**

91 2 07 034

Disclaimer

The findings in this report are not to be construed as an official Department of the Army position unless so designated by other authorizing documents.

Distribution Statement

Approved for public release; distribution is unlimited.

REPORT DOCUMENTATION PAGE

Form Approved
OMB No. 0704-0188

Public reporting burden for this collection of information is estimated to average 1 hour per response, including the time for reviewing instructions, searching existing data sources, gathering and maintaining the data needed, and completing and reviewing the collection of information. Send comments regarding this burden estimate or any other aspect of this collection of information, including suggestions for reducing this burden, to Washington Headquarters Service, Directorate for Information Operations and Reports, 1215 Jefferson Davis Highway, Suite 1204, Arlington, VA 22202-4302, and to the Office of Management and Budget, Paperwork Reduction Project (0704-0188), Washington, DC 20503.

1. AGENCY USE ONLY (Leave blank)		2. REPORT DATE 1990 December	3. REPORT TYPE AND DATES COVERED Final. 89 Aug - 90 Aug	
4. TITLE AND SUBTITLE Spectroscopic Analyses and Performance of Copper/Zinc Impregnated, Activated Carbons			5. FUNDING NUMBERS PR-1C162622A553E	
6. AUTHOR(S) Peterson, Erica, Morrison, Robert (CRDEC); Farris, Michelle, and Rossin, Joseph (GEO-Centers, Inc.)				
7. PERFORMING ORGANIZATION NAME(S) AND ADDRESS(ES) CDR, CRDEC, ATTN: SMCCR-PPP, APG, MD 21010-5423 GEO-Centers, Inc., Fort Washington, MD 20744			8. PERFORMING ORGANIZATION REPORT NUMBER CRDEC-TR-251	
9. SPONSORING/MONITORING AGENCY NAME(S) AND ADDRESS(ES)			10. SPONSORING/MONITORING AGENCY REPORT NUMBER	
11. SUPPLEMENTARY NOTES				
12a. DISTRIBUTION/AVAILABILITY STATEMENT Approved for public release; distribution is unlimited.			12b. DISTRIBUTION CODE	
13. ABSTRACT (Maximum 200 words) The U.S. Army Chemical Research, Development and Engineering Center is presently developing chromium-free carbons for collective and individual air purification systems. Spectroscopic analyses were performed on similar copper/zinc impregnated carbon samples prepared from a laboratory and production scale process. These samples displayed different levels of hydrogen cyanide protection. The difference in the performance was attributed to the location of copper within the carbon granules. In addition, copper was found to leach from the carbon granule during prolonged humid exposure. The leaching of copper resulted in a decrease in the level of hydrogen cyanide protection, as evidenced by premature breakthrough of a reaction product, cyanogen.				
14. SUBJECT TERMS Activated carbons			15. NUMBER OF PAGES 35	
			16. PRICE CODE	
17. SECURITY CLASSIFICATION OF REPORT UNCLASSIFIED	18. SECURITY CLASSIFICATION OF THIS PAGE UNCLASSIFIED	19. SECURITY CLASSIFICATION OF ABSTRACT UNCLASSIFIED	20. LIMITATION OF ABSTRACT UL	

Blank

PREFACE

The work described in this report was performed under Project No. 1C162622A553E, Collective Protection. This work was started in August 1989 and was completed in August 1990.

The use of trade names or manufacturers' names in this report does not constitute an official endorsement of any commercial products. This report may not be cited for purposes of advertisement.

Reproduction of this document in whole or in part is prohibited except with permission of the Commander, U.S. Army Chemical Research, Development and Engineering Center, ATTN: SMCCR-SPS-T, Aberdeen Proving Ground, MD 21010-5423. However, the Defense Technical Information Center and National Technical Information Service are authorized to reproduce the document for U.S. Government purposes.

This report has been approved for public release.

Acknowledgments

The author wishes to acknowledge David Tevault of the U.S. Army Chemical Research, Development and Engineering Center, Air Purification Branch for helpful discussion related to this work. The authors are also indebted to Robert Grue and J. Thomas Lynn for providing the hydrogen cyanide and cyanogen chloride breakthrough data.



Accession For	
NTIS GRA&I	<input checked="" type="checkbox"/>
DTIC TAB	<input type="checkbox"/>
Unannounced	<input type="checkbox"/>
Justification	
By	
Distribution/	
Availability Codes	
Dist	Avail and/or Special
A-1	

blank

CONTENTS

	Page
1. INTRODUCTION	9
2. EXPERIMENTAL METHODS	10
2.1 Materials.....	10
2.2 Spectroscopic Analysis	10
2.3 Adsorption Measurements of ASZ Carbons	11
2.4 Breakthrough Time Measurements	11
2.5 Humid Aging of ASZ Carbons	12
3. RESULTS	12
3.1 Impregnant Speciation	12
3.2 Impregnant Distribution	16
3.3 Adsorption Properties of ASZ Carbons	21
3.4 Reactive Properties of ASZ Carbons	21
3.5 Humid Aging of ASZ Carbons	23
4. DISCUSSION	23
4.1 Impregnant Speciation	23
4.2 Impregnant Distribution	27
4.3 Reaction Properties of ASZ Carbons	29
4.4 Humid Aging of ASZ Carbons	31
5. CONCLUSIONS	33
LITERATURE CITED	35

LIST OF FIGURES

	Page
1. XPS Spectra of the Copper 2p Photoelectron Region for Laboratory and Pilot Plant ASZ Carbon, and Copper Oxide	13
2. XPS Spectra of the Zinc 2p Photoelectron Region for Laboratory and Pilot Plant ASZ Carbon, and Zinc Oxide	14
3. XPS Spectra of the Zinc L ₃ M ₄₅ M ₄₅ Auger Region for Laboratory and Pilot Plant ASZ Carbon, and Zinc Oxide	15
4. BEI (a) and SEM (b) Images of a Bisected Laboratory ASZ Carbon Granule on Edge	17
5. BEI Image of a Bisected Laboratory ASZ Granule	18
6. BEI (a) and SEM (b) Images of a Bisected Pilot Plant ASZ Carbon Granule on Edge	19
7. BEI Showing Rod-like Crystals of Zinc Oxide at the External Surface of a Pilot Plant Prepared Carbon Granule	20
8. CFC-113 Adsorption Isotherms for Laboratory, Pilot Plant, and Aged (76 Days) Laboratory ASZ Carbons	22
9. XPS Cu/C Ratio Determined for Laboratory and Pilot Plant ASZ Carbon as a Function of Humid Aging Period	24
10. XPS Zn/C Ratio Determined for Laboratory and Pilot Plant ASZ Carbon as a Function of Humid Aging Period	25
11. Hydrogen Cyanide and Cyanogen Breakthrough Times (from a Hydrogen Cyanide Challenge) for Laboratory ASZ Carbon as a Function of the XPS Cu/C Ratio	26

LIST OF TABLES

	Page
1. Binding Energies for Elements Associated with ASZ Carbons	12
2. Quantitative EDS and XPS Analyses of Laboratory and Pilot Plant ASZ Carbon	21
3. Breakthrough Times for Impregnated Carbon Samples	23

Blank

SPECTROSCOPIC ANALYSES AND PERFORMANCE OF COPPER/ZINC IMPREGNATED, ACTIVATED CARBONS

1. INTRODUCTION

The current adsorbent (ASC whetlerite carbon) used in industrial and military air filters contains the impregnant hexavalent chromium. The hexavalent chromium is reported to provide protection against cyanide compounds¹⁻⁴. Because of the chromium, ASC Carbon is an EP Toxic Material under criteria established by the Environmental Protection Agency. As a result, costly procedures are necessary to dispose of the carbon filters. In addition, potential physiological risks are posed by the carcinogenic chromium to personnel manufacturing the carbon and the filters which contain the carbon, and to users of the filters should the filter become damaged in use. An investigation is currently underway to develop new impregnated carbons which do not contain hazardous impregnants for use in all military air filters.

During the formulation/optimization phase of the chromium-free carbon development program, a number of promising chromium-free formulations were prepared in the laboratory. Of these, a formulation of 6% copper, 0.05% silver, 6% zinc, and 3 to 4% triethylenediamine (TEDA) was determined to provide the best purification performance for chemical warfare protection. This material is designated ASZ carbon. While not quite as effective as ASC carbon in removing hydrogen cyanide from air, an acceptable level of performance was measured from the laboratory prepared sample. A mini-production lot of the ASZ carbon was then manufactured using pilot plant scale equipment. The production scale lot was found to provide inadequate protection against hydrogen cyanide because a reaction product of hydrogen cyanide, namely cyanogen, broke through the bed prematurely. Cyanogen is formed by the reaction of the copper(II) impregnant with hydrogen cyanide^{1,2}. Subsequent testing of the laboratory prepared carbon showed that after extended exposure to moist, warm air, premature cyanogen breakthrough also occurred.

The objective of this study was to characterize the two ASZ samples in an effort to:

- 1) Determine the difference in the physical properties which account for the difference in the performance between the laboratory and pilot plant prepared ASZ carbon samples.
- 2) Correlate the physical properties of the laboratory ASZ sample to its performance against a hydrogen cyanide challenge.
- 3) Determine the cause for the decreased hydrogen cyanide performance of the laboratory ASZ sample following prolonged humid aging.

2. EXPERIMENTAL METHODS

2.1 *Materials.*

Four activated, impregnated carbon samples were obtained from Calgon Corporation (Pittsburgh, PA). The first material was prepared in a laboratory scale batch and will be referred to as laboratory prepared ASZ. The second sample was prepared following a similar procedure as the first, but was prepared in a pilot plant scale batch. This material will be referred to as pilot plant ASZ. Both ASZ materials contained 6% (by weight) copper, 6% zinc, and 0.05% silver. The laboratory sample contained 4% triethylenediamine (TEDA) by weight while the pilot plant sample contained 3% TEDA by weight. The third impregnated carbon sample contained 12% copper by weight, with copper being the only impregnant. This material will be referred to as the copper reference sample. The fourth impregnated carbon sample contained 12% zinc by weight, with zinc being the only impregnant. This material will be referred to as the zinc reference sample. All samples were received as 12-30 mesh (U.S. Standard Sieve) granules.

The difference in the method of preparing the laboratory and the pilot plant ASZ sample was the drying procedure. The laboratory sample was dried in a tray in an electrically heated oven with the temperature programmed to increase gradually up to a peak of 175 °C over a period of several hours. The pilot plant sample was dried in a vibrating fluidized bed drier in which the carbon passed through heating zones of increasing temperature, again reaching a peak of 175 °C. This drier was fluidized by air directly heated by the combustion of natural gas, and thus the air contained products of the combustion reaction.

A copper oxide/zinc oxide carbon sample was prepared for use as a reference in the XPS studies. This sample was prepared by heating the pilot plant ASZ sample in hydrogen at 300 °C for 15 hours. This treatment results in the reduction of the zinc and copper complexes to the zero oxidation state. Following reduction, the sample was cooled to room temperature in flowing hydrogen. Once at room temperature, the hydrogen flow was discontinued and the sample was exposed to dry, flowing air. The sample was then heated from room temperature to 250 °C in one hour, with this temperature being maintained overnight. This procedure will result in the formation of copper and zinc oxides. The copper oxide/zinc oxide carbon sample will be referred to as reference copper oxide or reference zinc oxide sample.

2.2 *Spectroscopic Analysis.*

X-ray photoelectron spectroscopy (XPS) spectra were recorded using a Perkin-Elmer Phi 570 ESCA/SAM system employing MgK_α X-rays. Samples of the 12 - 30 mesh granules were analyzed for carbon, zinc, copper and oxygen. The concentration of silver was below the detection limit of the instrument, and therefore silver was not analyzed. Samples were dried in dry, flowing air for 4 hours

at room temperature prior to mounting and placing into the introduction chamber of the analysis unit. Once in the introduction chamber, the samples were evacuated (10^{-6} torr) overnight, then placed into the analysis chamber and analyzed. All binding energies are reported referenced to the carbon 1s photoelectron peak at 284.6 eV. Atomic ratios pertaining to elements of interest were determined by employing sensitivity factors supplied by the manufacturer.

Energy dispersive X-ray spectroscopy (EDS) was performed using a Tracor Northern 5700 EDS/WDS automation system interfaced with a JEOL 35CF scanning electron microscope. All data were recorded using 20 KeV electron accelerating voltage and count rates of 1500 to 2000 per second. EDS spectra were recorded for samples as-received (12-30 mesh granules) and for samples which had been bisected with a diamond knife. Six granules of each sample (laboratory and pilot plant ASZ) were analyzed in an effort to determine the homogeneity of the impregnation process in going from granule to granule, and to provide a statistical average of the results. In all cases, six different regions of a given granule were analyzed using an analysis area of approximately 150 by 190 μm . Detrimental effects of surface topography were minimized by taking into consideration the experimental geometry and the shape of the background X-ray envelope. Quantitative results from the six different analysis regions for the six granules (analyzed as-received and bisected) were averaged. Quantitative results were obtained by using the quantitation routine available with the instrument. In addition to the EDS analyses, each region was analyzed using scanning electron microscopy imaging in both secondary (SEM) and backscatter (BEI) modes.

2.3 *Adsorption Measurements of ASZ Carbons.*

Adsorption isotherms were recorded at 25 °C using 1,1,2 trichloro, 1,2,2 trifluoroethane (CFC-113) for the laboratory, pilot plant, and aged (76 days) laboratory ASZ carbon samples. Data were measured using a modified version of the closed-loop apparatus employed in previous studies⁵.

2.4 *Breakthrough Time Measurements.*

The reactivities of the carbon samples were determined by cyanogen chloride and hydrogen cyanide breakthrough tests. For both the hydrogen cyanide and cyanogen chloride breakthrough tests, the carbon was equilibrated prior to the reactive challenge with 30% RH air at 32 °C flowing at a linear velocity of approximately 10.0 cm/s overnight. This velocity corresponds to ca. 50,000 column volumes and is expected to approach equilibrium loading according to previous experience. The cyanogen chloride test was performed on a 3.0 cm deep bed at 80% RH, 24 °C with a feed concentration of 4 mg/l and a linear velocity of 9.6 cm/s. The breakthrough time is defined as the time at which the effluent cyanogen chloride concentration exceeds approximately 8 $\mu\text{g/l}$. The hydrogen cyanide breakthrough test was performed using a 3.0 cm deep carbon bed. Hydrogen

cyanide was challenged to the carbon bed with a concentration of approximately 10 mg/l in air at 24 °C (RH = 50%) flowing at a linear velocity of 6.2 cm/s. The breakthrough time of both cyanogen and hydrogen cyanide were recorded from the hydrogen cyanide challenge. The cyanogen breakthrough time is defined as the time at which the effluent concentration of cyanogen exceeds approximately 8 µg/l. The hydrogen cyanide breakthrough time is defined as the time at which the effluent concentration of hydrogen cyanide exceeds approximately 4 µg/l.

2.5 Humid Aging of ASZ Carbons.

Approximately 50 g each of the laboratory and pilot plant ASZ carbons were loaded into separate filter canisters. The filter canister is approximately 10 cm in diameter. Filling the canister with 50 g of carbon results in a bed approximately 1.0 cm deep. Once filled, the canisters were then placed in an environmental chamber which was designed to circulate humid air through the filled canisters. The humid aging was performed at 32 °C and 85 ± 5% RH air. Approximately one gram of each material was removed from the canister every seven days for surface analysis. Following removal, the sample was dried in dry, flowing air at room temperature for a minimum of four hours prior to analysis by XPS. This step was performed because it was felt that exposing the humidified sample to the high vacuum of the XPS analysis unit may alter the sample.

3. RESULTS

3.1 Impregnant Speciation.

Figure 1 compares the XPS spectra of the copper 2p photoelectron region of the ASZ samples (laboratory and pilot plant) to that of supported copper oxide/zinc oxide. Figure 2 compares the XPS spectra of the zinc 2p photoelectron region of the ASZ samples to that of the supported copper oxide/zinc oxide sample. The XPS spectra corresponding to the Zn L₃M₄₅M₄₅ auger line are reported in Figure 3 for the laboratory and pilot plant ASZ samples, and the supported copper oxide/zinc oxide sample. Binding energies for the elements of interest are reported in Table 1.

Table 1
Binding Energies for Elements Associated with ASZ Carbons

Element	Laboratory	Pilot Plant	CuO/ZnO
Cu 2p _{3/2}	934.2	934.4	933.9
Zn 2p _{3/2}	1022.2	1022.1	1022.4
Zn L ₃ M ₄₅ M ₄₅	266.0	265.7	265.7

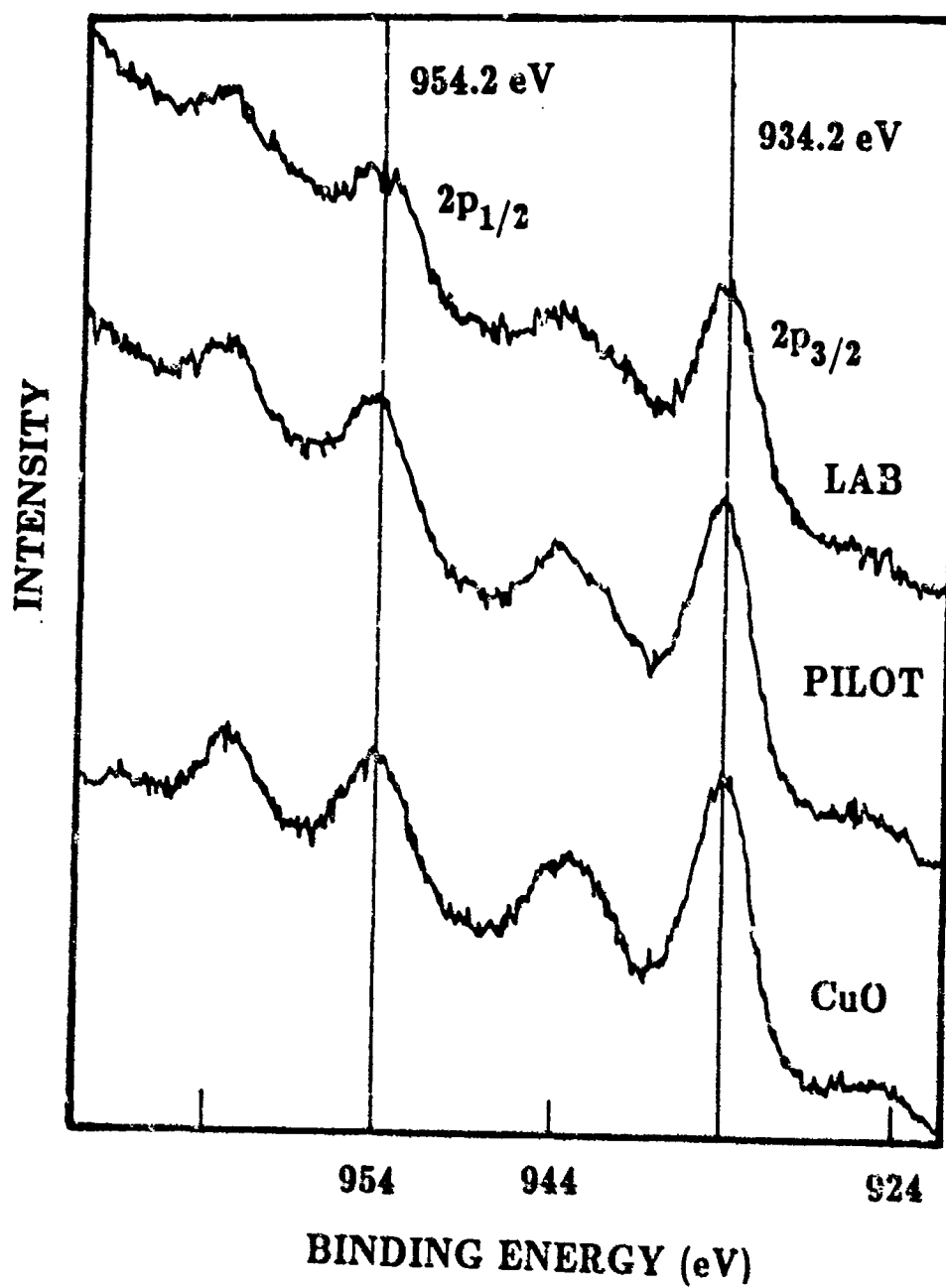


Figure 1. XPS Spectra of the Copper 2p Photoelectron Region for Laboratory and Pilot Plant ASZ Carbon, and Copper Oxide.

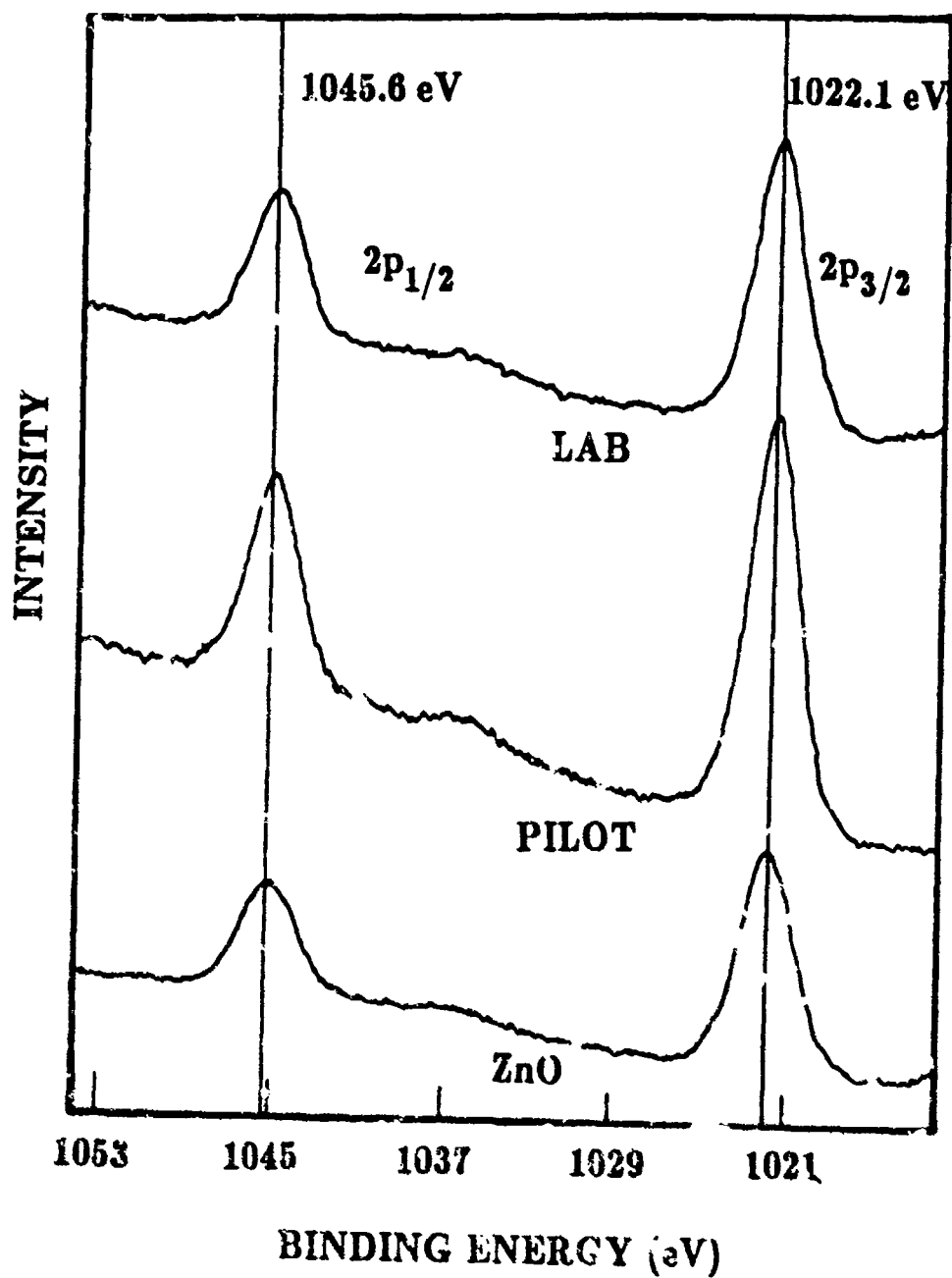


Figure 2. XPS Spectra of the Zinc 2p Photoelectron Region for Laboratory and Pilot Plant ASZ Carbon, and Zinc Oxide.

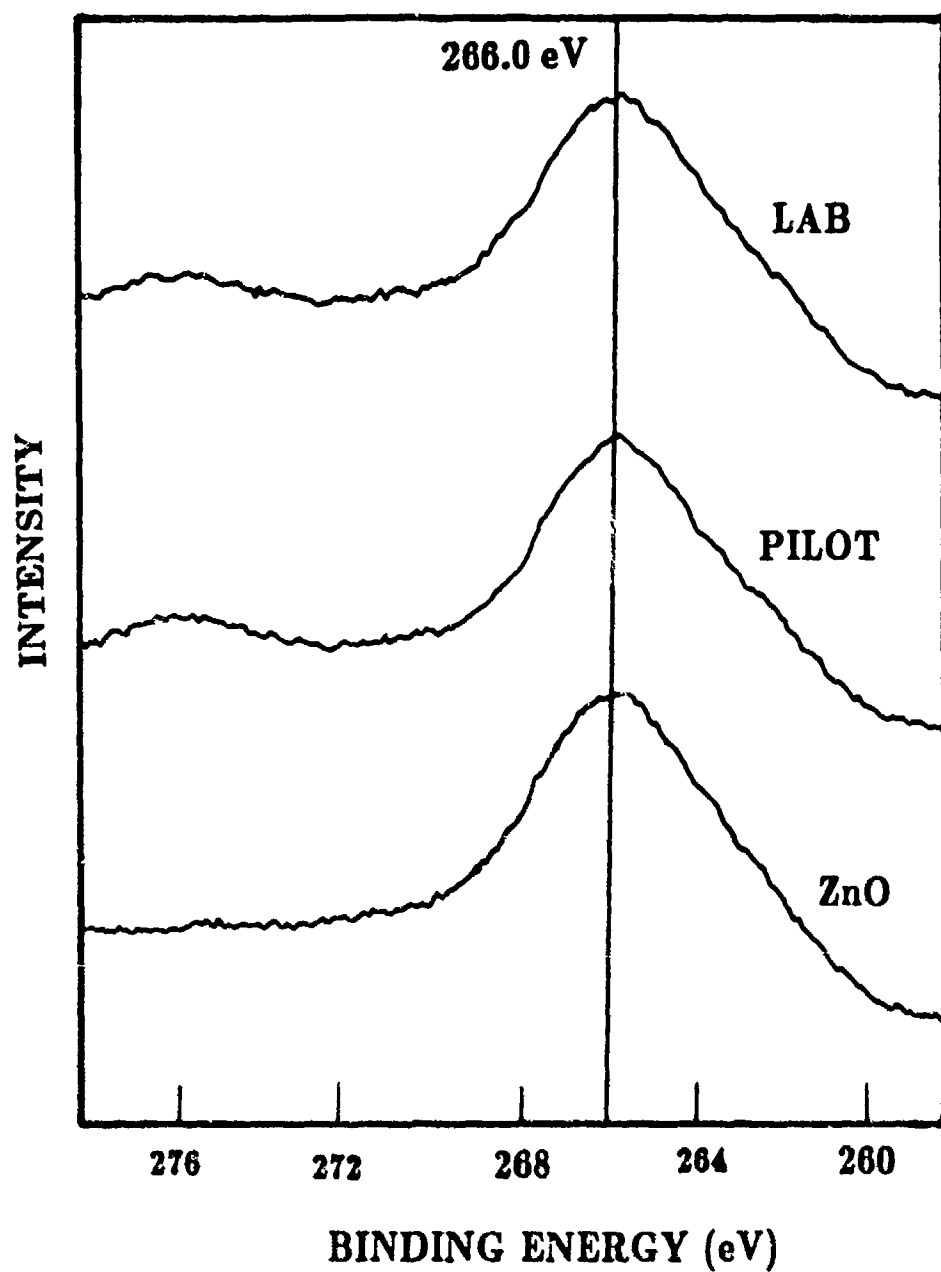
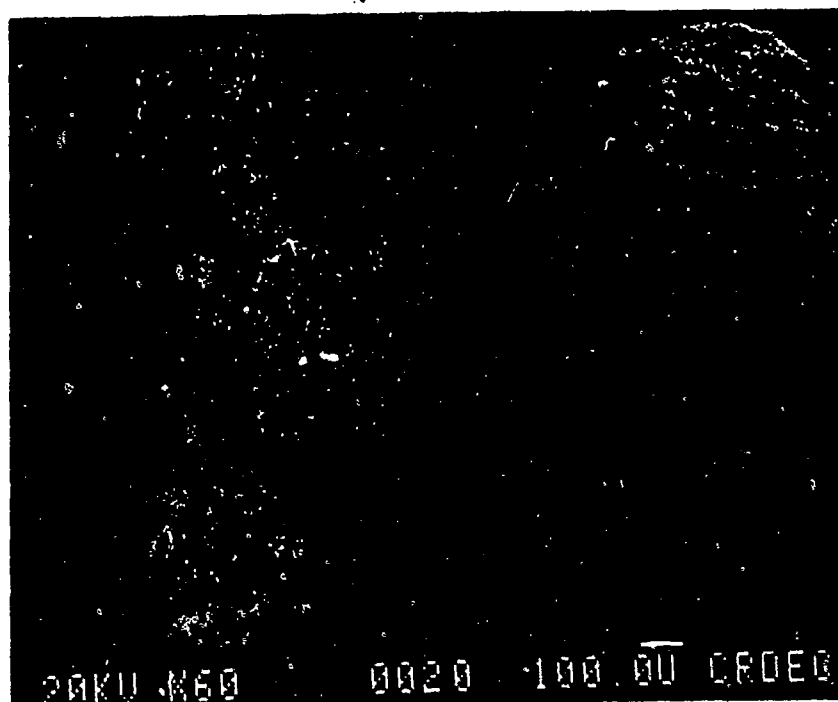


Figure 3. XPS Spectra of the Zinc L₂M₄₅M₄₅ Auger Region for Laboratory and Pilot Plant ASZ Carbon, and Zinc Oxide.

3.2 *Impregnant Distribution.*

Figure 4 shows an SEM and corresponding BEI of a representative laboratory carbon granule which has been bisected in half. A BEI image is similar to an SEM image, but highlights the heavy elements (copper and zinc in this case). The bisected surface is at the left of the image and can be seen as the dark surface in the BEI. The BEI image is presented edge-on in order to qualitatively illustrate the difference between the impregnant density present within the granule and at the external surface. A BEI of a bisected laboratory granule normal to the X-ray beam is shown in Figure 5. The thickness of the "ring" of metallic elements outlining the granule varies between 25 and 75 μm . Figure 6 shows an SEM and corresponding BEI of a representative pilot plant carbon granule which has been bisected. The dark region in the BEI corresponds to the bisected surface. Figure 7 shows a high magnification BEI image of the external surface of a pilot plant granule. EDS microbeam analysis indicate that the rod-like structures consist primarily of zinc. No large (greater than 0.1 μm) particles of copper were detected at the external surface of the granule.

Table 2 reports the quantitative XPS and EDS analyses, in the form of elemental (atomic) ratios, for the laboratory and pilot plant ASZ carbon samples. XPS data are reported for samples analyzed as granules. EDS data are reported for the external surface (referred to as surface in Table 2), and along the bisected surface (referred to as bulk in Table 2) of individual carbon granules. Quantitative values are reported relative to silicon because the detector associated with the instrument omits elements with molecular weights below sodium. A different production lot of base carbon was used in preparing the two ASZ samples. Because of this, the silicon content from each batch may be slightly different. Comparisons involving the metal to silicon ratios between the laboratory and pilot plant samples may therefore prove misleading. All data are reported for samples following 18 hours of humid aging, in order to be consistent with the reactive gas testing.



A

B

Figure 4. BEI (a) and SEM (b) Images of a Bisected Laboratory ASZ Carbon Granule on Edge. The bisected surface is at the left of the image.

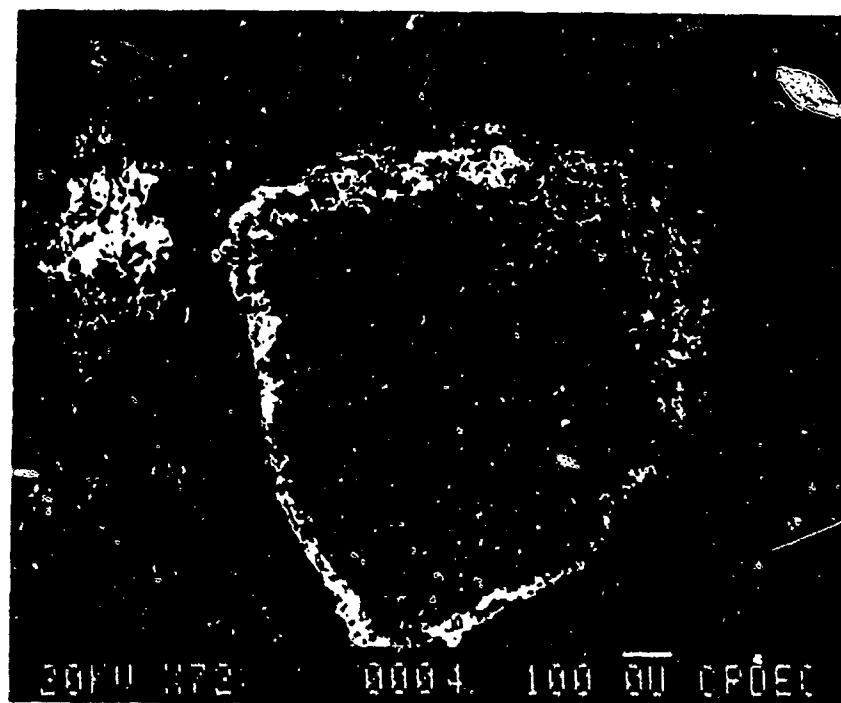
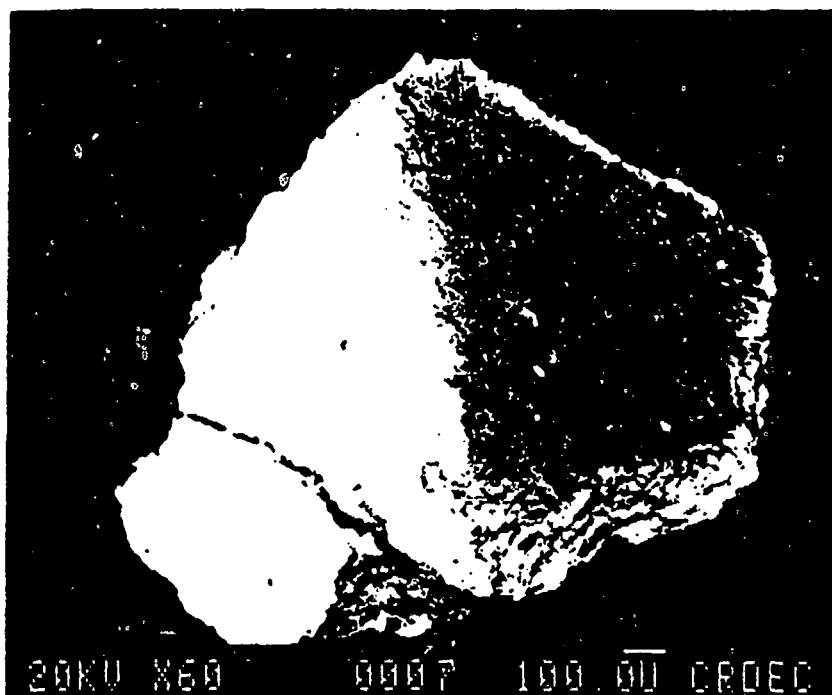
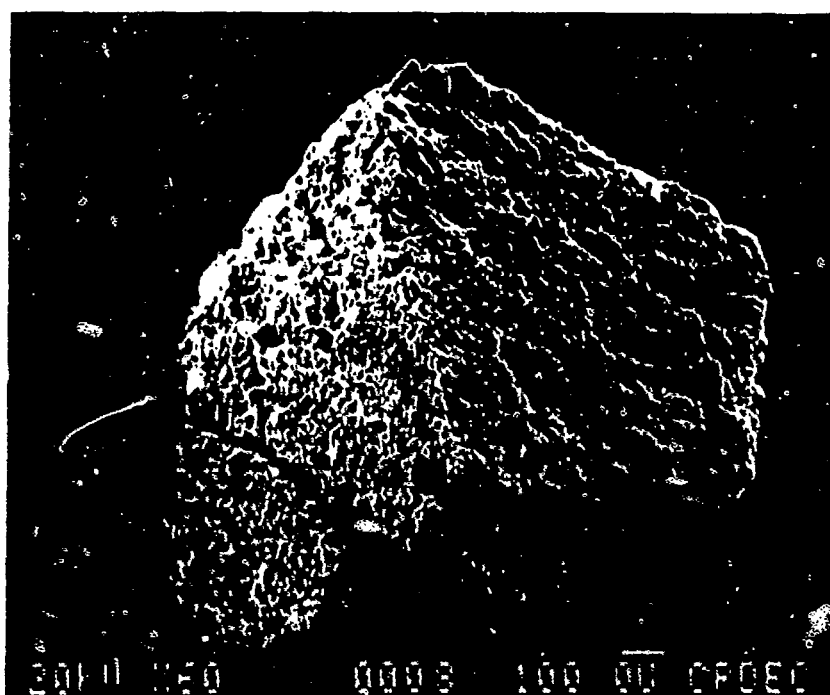


Figure 5. BEI Image of a Bisected Laboratory ASZ Granule. The bisected surface is perpendicular to the field of view.

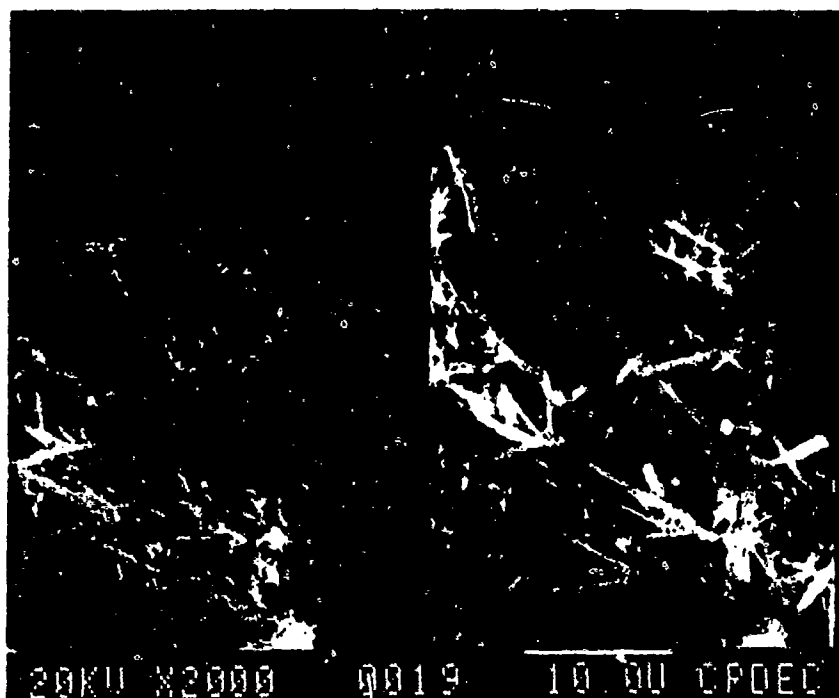


A



B

Figure 6. BEI (a) and SEM (b) Images of a Bisected Pilot Plant ASZ Carbon Granule on Edge. The bisected surface is at the right of the image.



S

♡

Figure 7. BEI Showing Rod-like Crystals of Zinc Oxide at the External Surface of a Pilot Plant Prepared Carbon Granule.

Table 2
Quantitative EDS and XPS Analyses of Laboratory and Pilot Plant ASZ Carbon

<u>EDS Analyses</u>				
	<u>Laboratory</u>		<u>Pilot Plant</u>	
	<u>Surface</u>	<u>Bulk</u>	<u>Surface</u>	<u>Bulk</u>
Cu/Si	3.02	2.69	3.33	1.33
Zn/Si	6.13	2.46	5.51	1.23
Cu/Zn	0.49	1.10	0.61	1.08

<u>XPS Analyses</u>				
	<u>Laboratory</u>		<u>Pilot Plant</u>	
	<u>XPS</u>	<u>CA *</u>	<u>XPS</u>	<u>CA</u>
Cu/C	0.031	0.013	0.069	0.013
Zn/C	0.162	0.013	0.174	0.013
Cu/Zn	0.191	1.03	0.40	1.03

* Chemical Analysis

3.3 *Adsorption Properties of ASZ Carbons.*

Shown in Figure 8 are the results of the isotherm measurements of CFC-113 adsorbed on the laboratory, pilot plant and aged (76 days) laboratory ASZ carbon samples. The results show that the adsorption capacity of the pilot plant sample is slightly lower than (or at best equal to) the laboratory sample over the range of concentrations measured. The difference in the capacity between these two samples is minimal. There is a loss in the adsorption capacity of the laboratory sample following 76 days of humid aging, however, the change is not large enough to dramatically affect the adsorption equilibria.

3.4 *Reactive Properties of ASZ Carbons.*

Table 3 reports the hydrogen cyanide, cyanogen (from a hydrogen cyanide feed) and cyanogen chloride breakthrough times for the laboratory and pilot plant ASZ carbon samples, and carbon samples consisting of zinc only, copper only, and the laboratory sample following 76 days of humid aging. The breakthrough times for ASC whetlerite are reported for comparison.

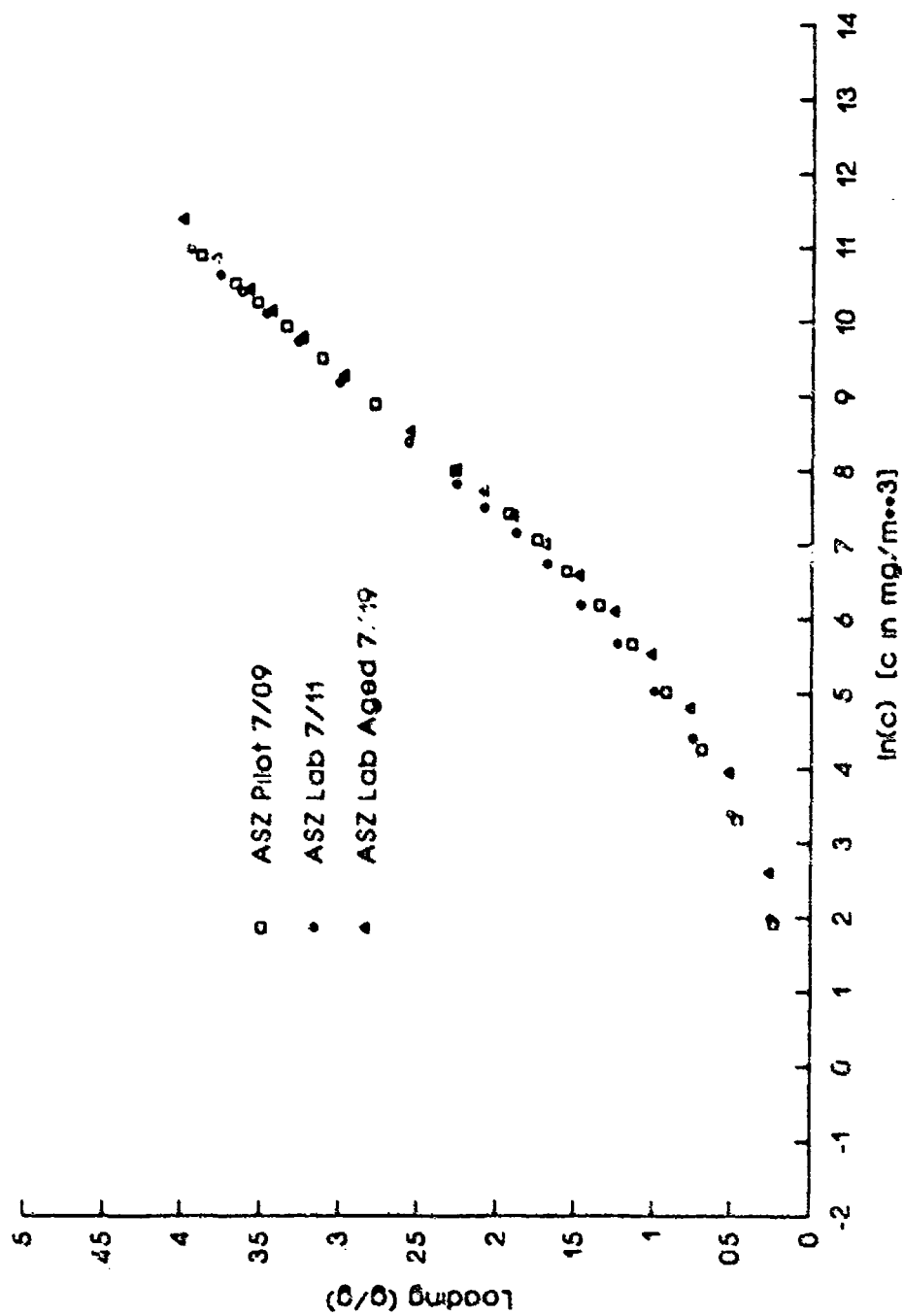


Figure 8. CFC-113 Adsorption Isotherms for Laboratory, Pilot Plant, and Aged (76 Days) Laboratory ASZ Carbons.

Table 3
Breakthrough Times for Impregnated Carbon Samples

<u>Sample</u>	<u>Breakthrough Time (Min)</u>		
	<u>HCN</u>	<u>(CN)₂</u>	<u>ClCN</u>
Laboratory	32.2±0.7	17.9±0.5	58.0
Pilot	26.2±0.6	6.5±1.1	47.1
Supported Zn	18.3±1.3	— [†]	N/A
Supported Cu	20.0±1.3	2.6±1.2	N/A
Aged Laboratory	24.9±1.3	4.3±1.2	N/A
ASC	36.5±1.8	33.7±2.3	37.8

[†] Breakthrough concentration not exceeded.

3.5 *Humid Aging of ASZ Carbons.*

Figures 9 and 10 report the XPS copper-to-carbon and zinc-to-carbon atomic ratios, respectively, for laboratory and pilot plant prepared ASZ carbon as a function of the humid aging time. Data reported in these figures are for carbon samples analyzed as granules. Figure 11 reports the hydrogen cyanide and cyanogen (from a hydrogen cyanide challenge) breakthrough times for the laboratory prepared ASZ carbon sample as a function of the superficial copper-to-carbon ratio. The superficial copper-to-carbon ratio was determined by XPS analysis of the sample as a granule. This ratio was varied by the humid aging process. Data reported in Figure 12 corresponds to 1, 7, 34 and 76 days of humid aging.

4. DISCUSSION

4.1 *Impregnant Speciation.*

XPS spectra are reported for the purpose of identifying the oxidation state and/or speciation of the copper and zinc impregnants. The quantity of silver associated with the samples (less than 0.05% by weight) was below the detection limits of the instrument and therefore no data pertaining to the silver are reported. The XPS spectra presented in Figure 1 indicates that the vast majority of copper is in the +2 oxidation state for both the laboratory and pilot plant ASZ samples. This is based on the binding energy of the copper and the presence of the satellite shake-up peaks at approximately 944 and 959 eV⁶. The copper 2p XPS spectra corresponding to both the ASZ samples are similar, indicating a common copper speciation for both samples. The copper 2p XPS spectra pertaining to reference copper(II) oxide is reported for comparison. The binding energy of 933.9 eV reported for copper oxide is consistent with values reported in the literature^{6,7}. The

Atomic Ratios as Determined by XPS

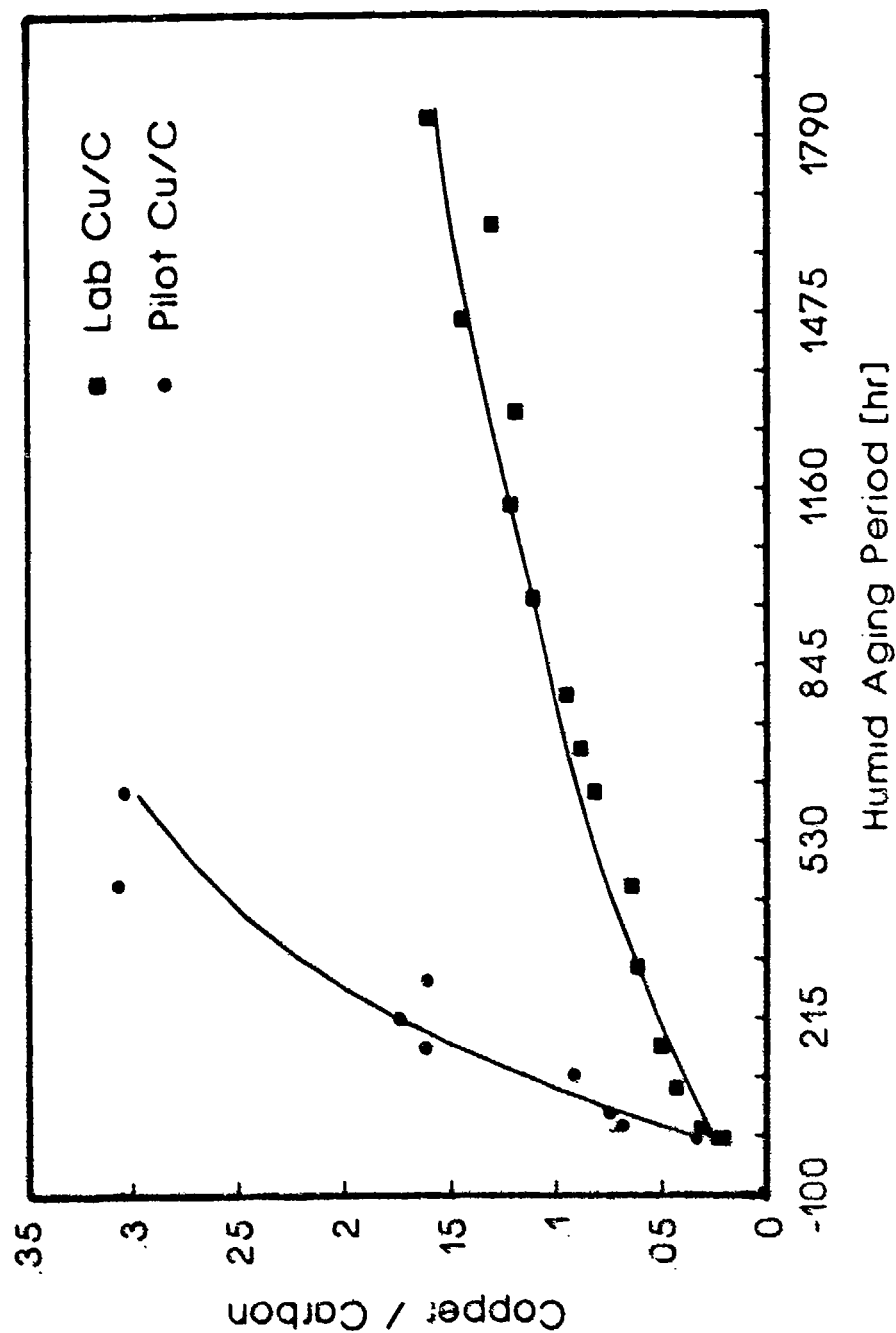


Figure 9. XPS Cu/C Ratio Determined for Laboratory and Pilot Plant ASZ Carbon as a Function of Humid Aging Period.

Atomic Ratios as Determined by XPS

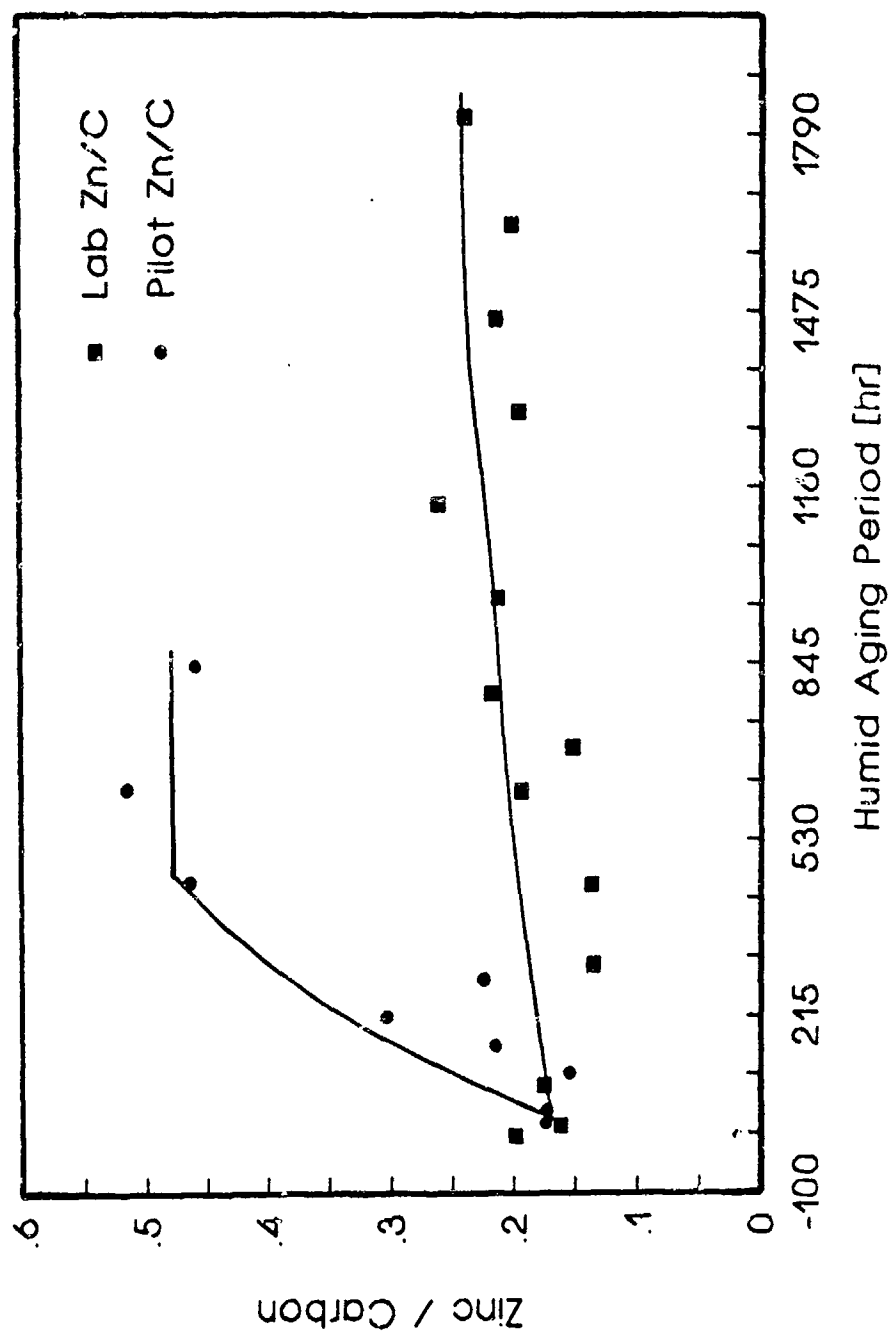


Figure 10. XPS Zn/C Ratio Determined for Laboratory and Pilot Plant ASZ Carbon as a Function of Humid Aging Period.

Effects of Surface Copper on Breakthrough Times

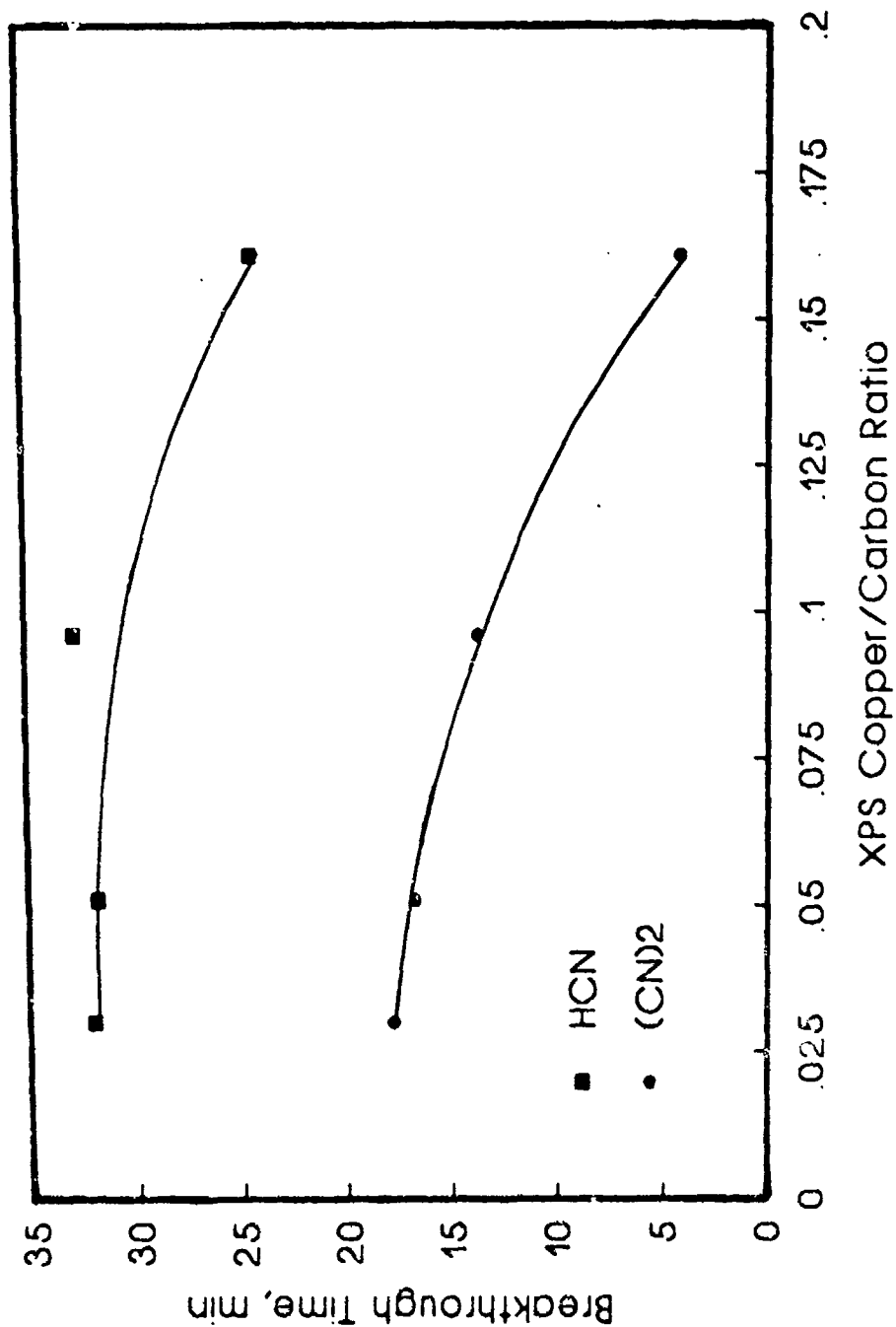


Figure 11. Hydrogen Cyanide and Cyanogen Breakthrough Times (from a Hydrogen Cyanide Challenge) for Laboratory ASZ Carbon as a Function of the XPS Cu/C Ratio.

binding energy of the reference copper(II) oxide sample is at a slightly lower binding energy than that of the ASZ samples. There are also some slight differences in the shape of the shake-up peaks. It is possible that the copper associated with the ASZ samples is in the form of copper oxide. The differences in the XPS spectra may be the result of an interaction between copper oxide and zinc oxide, or differences resulting from the preparation of the supported copper(II) oxide sample. However, the XPS data are inclusive as to the speciation of copper on the ASZ carbon samples.

XPS data reported in Figure 2 compare the zinc 2p photoelectron peaks corresponding to the laboratory and pilot plant ASZ carbons, and the reference zinc oxide sample. Note from the figure that all peaks are present at approximately the same binding energy. The position of the zinc $2p_{3/2}$ photoelectron peak is relatively invariant to the oxidation state of zinc⁵. For example, the binding energy of the $2p_{3/2}$ photoelectron peak for zinc metal is reported to be between 1021.4 and 1022.1 eV, while that of zinc oxide is reported to be between 1021.7 and 1022.5 eV. As a result, the zinc 2p photoelectron peak provides little information pertaining to the oxidation state of zinc. The $L_{3}M_{45}M_{45}$ zinc auger line is often used to determine the oxidation state and/or speciation of zinc containing compounds, as the position of this peak is more sensitive to changes in the speciation and/or oxidation state of zinc. As shown in Figure 3, the position and shape of the zinc auger line is similar for all three samples illustrated in the figure. These data indicate that zinc is in the +2 oxidation state, possibly existing as zinc oxide for both ASZ samples.

From the XPS spectra reported in Figures 1 through 3, no difference in the impregnant speciation between the laboratory and pilot plant sample is apparent. XPS spectral data suggests that the zinc associated with the ASZ carbon samples is in the form of zinc oxide. Copper associated with the ASZ samples is in the +2 oxidation state.

4.2 *Impregnant Distribution.*

The BEI reported for the bisected granules (both laboratory and pilot plant, see Figures 4, 5 and 6) indicate that at least one of the impregnants is concentrated near the external surface of the granule. The "ring" of impregnants near the external surface of the granule varied between 10 and 75 μm in thickness. Examination of the external surface of laboratory and pilot plant granules revealed high concentrations of rod-like structures approximately $0.5 \times 10 \mu\text{m}$ consisting primarily of zinc (see Figure 7). No large copper particles were detected, suggesting that the copper dispersion is much better than that of zinc. These data clearly show that zinc is highly concentrated and poorly dispersed near the external surface of both the pilot plant and laboratory ASZ samples.

Quantitative EDS and XPS analyses may be used to provide information regarding the radial distribution of the metal impregnants. EDS provides a

chemical analysis to a depth of approximately 0.5 μm over the analysis area while XPS provides a chemical analysis of the outer 30 to 50 Å of the surface exposed to the x-ray source. XPS probes the outer few atoms near the external surface while the EDS will probe a greater distance into the sample. For both the laboratory and pilot plant ASZ samples, the Zn/Si ratio determined by EDS is approximately 3 to 5 times greater at the external surface of the granule relative to that of the bulk (see Table 2). The Zn/C ratio determined at the external surface of the granule by XPS is also significantly greater (approximately 13 times) than that obtained from chemical analysis for both the laboratory and pilot plant samples. This was to be expected since large zinc particles were detected at the external surface. These data are consistent with the BEI surface images which indicate that zinc is poorly dispersed at the external surface of the granule for both the laboratory and pilot plant sample.

Large copper particles were not detected at the external surface of either granule. Therefore, EDS and XPS analyses will be the only source of information regarding the distribution of copper within the granule. The copper distribution among the two ASZ samples was different. For the laboratory sample, the Cu/Si ratio at the external surface (determined by EDS) was similar to that determined from analysis of the bulk. Also, the Cu/C ratio (determined by XPS) was approximately 2.5 times greater than that obtained from chemical analysis. Shannon et al.⁸ have used XPS to indicate whether an impregnant is accumulated at the external surface of the support or whether the impregnant is uniformly distributed within the support. The authors did this by comparing the metal concentration determined by XPS to that determined by chemical analysis (CA). XPS/CA ratios of approximately one suggested that the impregnant is uniformly distributed throughout the support, while ratios of about 30 suggested that the impregnant is exclusively located at the external surface. EDS and XPS data reported here suggest that the copper is not concentrated at the external surface of the laboratory sample, and the copper may be uniformly distributed within the granule. For the pilot plant sample, the Cu/Si ratio determined by EDS is almost three times greater than that of the bulk, and the Cu/C ratio determined by XPS is approximately six times greater than that determined by chemical analysis. These data indicate that a larger fraction of the copper may be concentrated in the superficial regions of the granule relative to the laboratory sample.

Care should be taken in gauging the magnitude of the elemental ratios determined by both EDS and XPS. This is because of the nonhomogeneity of the external surface (large zinc oxide particles). Since both the EDS and XPS techniques analyze a very small distance into the sample (relative to the particle diameter), not all the zinc at the external surface will be analyzed. Also, the zinc particles may be shielding copper from detection. Consequently, elemental ratios computed upon analysis of the external surface with respect to zinc are conservative.

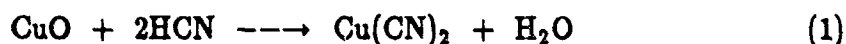
Spectroscopic analyses of the two ASZ carbon samples indicates that a large fraction of zinc is present at the external surface of the granules. The zinc exists as

large particles of zinc oxide. The copper associated with the laboratory sample is not concentrated at the external surface and may be uniformly distributed within the granule. The copper associated with the pilot plant sample is more concentrated at the external surface than the laboratory sample.

Both ASZ samples were prepared by a simultaneous impregnation with a zinc and copper carbonate solution. The impregnation process did not result in the accumulation of copper particles at the external surface of the granule; however, the process did accumulate zinc over regions very near the external surface of the granule. It is possible that either the zinc did not disperse well during the impregnation process, or that during the drying procedure the zinc migrated and accumulated at or near the external surface of the carbon granules.

4.3 *Reaction Properties of ASZ Carbons.*

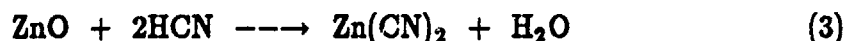
The hydrogen cyanide and cyanogen breakthrough times from a hydrogen cyanide challenge are reported for the copper reference and the zinc reference impregnated carbon samples for the purpose of characterizing the reactions which occur over the two metals. The hydrogen cyanide breakthrough time of the copper reference carbon was about one-third less than that of the ASZ sample. The difference is likely the result of a reduced copper dispersion when 6% of the zinc is replaced by an additional 6% copper. The cyanogen breakthrough time from the hydrogen cyanide challenge demonstrates that a copper-only formulation provides virtually no protection against a hydrogen cyanide challenge. This result is not surprising based on the reported reaction sequence involving copper oxide^{1,2}:



The reduction of the copper cyanogen complex to copper cyanide is very fast. The reason for the finite cyanogen breakthrough time is that a portion of the product cyanogen is adsorbed onto the carbon support.

For the zinc reference sample, the breakthrough time recorded for hydrogen cyanide is about one third less than that reported for the laboratory ASZ sample. The difference in performance is likely due to a reduced zinc dispersion when 6% of the copper is replaced with an additional 6% zinc. The cyanogen (from a hydrogen cyanide challenge) breakthrough concentration was not exceeded for the zinc reference formulation, however a trace of cyanogen was observed in the effluent. Barton and Smith⁹ have reported the formation of cyanogen upon exposing unimpregnated carbon to a hydrogen cyanide challenge. They attributed the formation of cyanogen to the reaction of hydrogen cyanide with impurities in the carbon. The cyanogen detected from the hydrogen cyanide challenge may be due to the reaction of the hydrogen cyanide with impurities in the carbon, similar to what Barton and

Smith observed. The lack of cyanogen production from the zinc only formulation was to be expected based on the reported reaction involving zinc oxide and hydrogen cyanide¹⁰:



From the data reported in Table 3, the zinc reference material, laboratory ASZ carbon and ASC whetlerite were the only samples to provide a threshold protection against a hydrogen cyanide challenge. Neither experimental material possessed a level of performance equivalent to that of ASC whetlerite. What is surprising is that while both the laboratory and pilot plant ASZ samples were of a similar metal composition, their performance against a hydrogen cyanide challenge is significantly different. Also, aging of the laboratory sample results in a significant decrease in its protection capability.

The difference in the hydrogen cyanide performance of the two ASZ samples may be due to either an adsorption or reaction effect. A change in the adsorption capacity of the carbon resulting from the impregnant location could adversely effect the capacity for cyanogen adsorption, leading to its premature breakthrough, as was observed upon challenging the pilot plant sample with hydrogen cyanide (Table 3). However, CFC-113 isotherms (Figure 8) demonstrate that the adsorption capacity of both materials is similar. Therefore, the difference in the performance of the laboratory and pilot plant samples is attributed to a reaction effect resulting from the difference in the copper distribution.

To address this problem of premature breakthrough of cyanogen from a hydrogen cyanide challenge, elimination of the copper from the impregnant formulation would, in some applications, be a viable alternative. However, the specific adsorbent under development is required to provide protection against a broad spectrum of toxic agents. The copper oxide is effective in providing reactivity toward militarily important toxic chemicals such as arsine, chlorine, and acid gas producers such as phosgene¹¹. Therefore, elimination of the copper from the adsorbent used for military application does not appear to be a viable option. The zinc is included in the formulation to provide reactivity toward hydrogen cyanide without the formation of cyanogen, to act in concert with copper and TEDA to provide cyanogen chloride filtration, and to act as an acid gas sink. Thus, inclusion of both the copper and the zinc is considered to be important to provide a high level of filtration performance against a broad spectrum of military toxic agents. Since the copper needs to be included in the formulation and the formation of cyanogen from a hydrogen cyanide challenge must be minimized, control of the dispersion of the impregnants could provide the selective reactivity required. The zinc must be impregnated on the carbon so as to be much more accessible than the copper to the hydrogen cyanide challenge.

One method of making the zinc more accessible to the reactant is to deposit high concentrations of zinc at the external surface of the carbon granule while uniformly distributing the copper throughout the interior of the granule. In this manner, diffusional resistances will make the copper less accessible and the hydrogen cyanide reaction will occur predominantly over zinc. Diffusional resistances involving the reaction of light gases over ASC whetlerite have been reported by Friday¹². The laboratory ASZ sample possessed a highly concentrated zinc phase near the external surface of the granule and a copper phase evenly distributed

throughout the granule. The breakthrough times for this novel copper/zinc formulation for hydrogen cyanide and cyanogen from a hydrogen cyanide challenge, and cyanogen chloride are reported in Table 3. The level of protection provided by the laboratory sample against a hydrogen cyanide challenge is less than that of ASC-TEDA but superior to that of the copper-only sample and the pilot plant ASZ sample (based on the cyanogen breakthrough time). The reason for the poor performance of the pilot plant sample and the improved performance of the laboratory sample against a hydrogen cyanide challenge is attributed to the copper location. The pilot plant sample possessed a greater fraction of copper near the external surface of the granule. Because of this, the reactions involving hydrogen cyanide over zinc and copper would proceed at similar rates, leading to the observed premature cyanogen breakthrough. For the laboratory sample, the copper distribution was shown to be nearly uniform, and the hydrogen cyanide will react preferentially with zinc due to its accessibility. Any reaction occurring over copper will be less significant, and the cyanogen produced would be adsorbed by the carbon support. As the zinc becomes consumed by the reaction, the reaction of hydrogen cyanide occurring over copper becomes more significant, leading to the cyanogen breakthrough.

We were unable to obtain a sample in which both copper and zinc were homogeneously distributed throughout the carbon granule. However, a sample in which both the copper and zinc were present in large concentrations at the external surface of the granule was prepared by aging the laboratory sample in a humid environment. The hydrogen cyanide and cyanogen breakthrough data from a hydrogen cyanide challenge obtained for this sample demonstrate the need to segregate the copper and zinc impregnants. For this sample, the protection against hydrogen cyanide (cyanogen breakthrough) is almost nonexistent. With both the copper and zinc equally accessible to the hydrogen cyanide, the reaction occurring over copper proceeds at an appreciable rate, leading to the formation of large quantities of cyanogen.

The cyanogen chloride performance is significantly better in the case of the laboratory sample. This may be a result of the better copper dispersion, but the sample also possessed more TEDA, which plays a role in the destruction of cyanogen chloride.

4.4 *Humid Aging of ASZ Carbons.*

A requirement of an impregnated carbon is that it be able to provide protection following an extended period of environmental exposure. The conditions of the humid aging experiment conducted in this study simulate environmental exposure at extreme conditions. Both the laboratory and pilot plant samples were characterized by XPS for changes in the impregnant oxidation state and changes in the surface composition as a function of humid exposure. Hydrogen cyanide breakthrough tests were also performed (laboratory sample only) at different humid exposure periods. Results of the XPS analysis revealed that no change in the impregnant oxidation state occurred as a result of the humid exposure. Spectra of the weathered samples were similar to those of the unweathered samples.

A change in the impregnant surface composition with increased weathering was evident. Note from Figure 9 that the Cu/C ratio increases with exposure time for both ASZ samples. These data indicate that copper is migrating from within the carbon granule to the external surface. The rate of increase in the surface copper concentration is greater for the pilot plant sample than for the laboratory

sample. This would suggest that there is more copper near the external surface of the pilot plant sample than the laboratory sample. By having more copper near the external surface, the rate of migration and accumulation at the external surface would be greater because of the shorter path length. This is consistent with the EDS and XPS analyses, which indicated that the pilot plant sample had a greater concentration of copper near the external surface than did the laboratory sample.

Migration of the zinc was also evident, although there was a significant fraction of zinc at the external surface of the freshly prepared ASZ samples. Note from Figure 10 that the Zn/C ratio increases sharply with time for the pilot plant sample but increases more slowly in the case of the laboratory sample. These data would suggest that any zinc below the external surface has begun to migrate towards the external surface.

The hydrogen cyanide and cyanogen breakthrough times (from a hydrogen cyanide challenge) are reported in Figure 11 as a function of the XPS Cu/C ratio. As the figure shows, both the hydrogen cyanide and cyanogen breakthrough times decrease as the copper concentration at the external surface of the granule is increased. CFC-113 isotherms comparing the unaged and aged (76 days) laboratory carbons indicates that the migration of the copper has reduced the adsorption capacity; however, the changes are not dramatic enough to cause the large decrease in the performance. These data support the proposed reaction hypothesis. As the copper migrates to the external surface, it becomes more accessible to the hydrogen cyanide. Hence, the reaction of hydrogen cyanide over copper becomes appreciable, and the rate of cyanogen production increases, resulting in premature breakthrough. The hydrogen cyanide breakthrough time also decreases, although not as significantly as the cyanogen time. This may be the result of a decreased impregnant dispersion, or a decrease in the adsorption capacity for hydrogen cyanide resulting from pore blockage.

5. CONCLUSIONS

1. Zinc is highly concentrated at and near the external surface of both ASZ samples, in the form of large zinc oxide particles.
2. Copper is concentrated at the external surface of the pilot plant sample, although not to the extent of zinc. For the laboratory sample, the copper was not concentrated at the external surface of the granule.
3. Since zinc is more concentrated at the external surface of the granule than copper, the mechanism responsible for the surface migration of zinc during the sample preparation must be more active than that of copper.
4. The adsorption properties of the laboratory and pilot plant ASZ samples are similar.
5. The difference in the performance of the laboratory and pilot plant ASZ samples results from the copper location within the granules.
6. Upon humid aging of both ASZ samples, copper and zinc migrate and accumulate at the external surface of the granules. The rate of migration is greater in the case of the pilot plant sample. The migration of copper results in decreasing the protection capabilities of the laboratory sample.

Blank

LITERATURE CITED

- 1) Brown, P. N., Jayson, G. G., Thompson, G. and Wilkinson, M.C., "Adsorption Characteristics of Impregnated Activated Charcoal Cloth for Hydrogen Cyanide", *J. Coll. Int. Sci* Vol. 116, p 211 (1987).
- 2) Brown, P. N., Jayson, G. G., Thompson, G. and Wilkinson, M.C., "Effect of Ageing and Moisture on the Retention of Hydrogen Cyanide by Impregnated Activated Charcoals", *Carbon* Vol. 27, p 821 (1989).
- 3) Hammarstrom, J. and Sacco, A., "Investigation of Deactivation Mechanisms of ASC Whetlerite Charcoal", *J. Catal.* Vol. 112, p 267 (1988).
- 4) Ross, M. M., Colton, R. J. and Dietz, V. R., "The Study of Whetlerite Surfaces by X-ray Photoelectron Spectroscopy", *Carbon* Vol. 27, p 426 (1989).
- 5) Mahle, J. J., Buettner, L. D. and Friday, D. K., "Batch Adsorption: Equilibria and Rate Processes", in *Proc. 1989 Conf. Chem. Def.*, in press.
- 6) Wagner, C. D., Riggs, W. M., Davis, L. E., Moulder, J. F. and Muilenberg, G. E. (eds.), *Handbook of X-Ray Photoelectron Spectroscopy*, Perkin-Elmer Corp., Eden Praire, Minn. 1979.
- 7) Rossin, J. A., "XPS Surface Studies of Activated Carbon", *Carbon* Vol. 27, p 611 (1989).
- 8) Shannon, R. D., Vadrine, J. C., Naccache, C. and Lefebvre, F., "Surface Studies of Transition Metal Impregnated Zeolites", *J. Catal.* Vol. 88, p 431 (1984).
- 9) Barton, S. S. and Smith, R. J., "The Reaction of Hydrogen Cyanide and Cyanogen with Unimpregnated, Activated Carbon", Presented at the 19th Biennial Conf. on Carbon, Penn State Univ., Univ. Park, PA (1989).
- 10) Smisek, M. and Cerny, S., *Active Carbon*, Elsevier Pub. Co., New York, NY, p 188 (1970).
- 11) Grabenstetter, R. J. and Blacet, F. E., "Impregnation of Charcoal", Chapter 4 in Sum. Tech. Report Div. 10, Natl. Def. Res. Comm., Mil. Prob. Aerosols and Nonpersistent Gases, Vol. 1 (1946).
- 12) Friday, D. K., "The Breakthrough Behavior of a Light Gas in a Fixed Bed Adsorptive Reactor", *AIChE Symp. Ser. #264*, Vol. 84, p 89 (1988).